Supplemental Material

December 5, 2017

Further Observational Details

Selection in SDSS-III BOSS of J1100-0053

SDSS J1100-0053.71-005304.5 was first detected by the ROSAT and appears in the All-Sky Survey Bright Source Catalogue [RASS-BSC; 6, 35]. J1100-0053 was then imaged by the Sloan Digital Sky Survey (SDSS) and satisfied a number of spectroscopic targeting flags[1] making it a quasar target. A spectrum was obtained on MJD 51908 (Plate 277, Fiber 212) and the spectrum of a $z = 0.378$ quasar was catalogued in the SDSS Early Data Release [28, 33]. The physical properties of J1100-0053, derived from the MJD 51908 spectrum and using the methods in Shen et al. [30], are given in Table 1.

The second epoch spectrum is from the SDSS-III Baryon Oscillation Spectroscopic Survey [BOSS; 8] and shows the downturn at $\lesssim$4300Å . SDSS-III BOSS actively vetoed low-z QSOs [27], and it was due to J1100-0053 being selected as an ancillary target via a white dwarf program [14, 15] that a second spectral epoch was obtained. Since J1100-0053 was not a BOSS QSO target, it is not subject to the "blue offset", see Margala et al. [18].

A third epoch spectrum was obtained from the Palomar Hale 5m telescope using the DBSP instrument. Two exposures of 600s+300s were taken in good conditions. Features to note include the continuum straddling Mg II being blue in the 2017 spectrum, as it was for the SDSS spectrum in 2000, as opposed to red, as it was for the BOSS spectrum in 2010.

J1100-0053 is in Data Release 3 (DR3) of the Dark Energy Camera Legacy Survey (DECaLS), where there are 8, 3 and 9 exposures in the g, r and z-band respectively. The g- and r-band observations are separated by roughly a year, ($56707 \leq g_{\mathrm{MJD}} \leq 56727$ and $56367 \leq r_{\mathrm{MJD}} \leq 56367$). The z-band observations span almost 3 years ($56383 \leq z_{\mathrm{MJD}} \leq 57398$).

Selection in NEOWISE-R of J1100-0053

WISE W1 and W2 lightcurves for ∼200,000 SDSS spectroscopic quasars were obtained. These light curves span from the beginning of the WISE mission (2010 January) through the first-year of NEOWISE-R operations (2014 December). The W1/W2 light curves are obtained by performing forced photometry

[1] SERENDIP_BLUE, ROSAT_D, ROSAT_C, ROSAT_B, QSO_SKIRT, ROSAT_A, see Stoughton et al. [32] and Richards et al. [26] for flag descriptions.

Quantity	Value
SDSS name	J1100-0053.71-005304.5
R.A. / deg	165.240463
Declination / deg	-0.884586
redshift, z	0.3778±0.0003
$M_i(z = 2)$ / mag	-24.48
log $(L_{\mathrm{bol}}/\mathrm{ergs}^{-1})$	45.78±0.02
log $(M_{\mathrm{BH}}/M_{\odot})$	8.83±0.14
Eddington ratio	0.070

Table 1: Physical properties of J1100-0053 using the methods from Shen et al. [30].

at the locations of DECam-detected optical sources [17, 20, 21]. This forced photometry is performed on time-resolved unWISE coadds [17], each of which represents a stack of $\sim$12 exposures. A given sky location is observed by WISE for $\sim$1 day once every six months, which means that the forced photometry light curves typically have four coadd epochs available. Coadd epochs of a given object are separated by a minimum of six months and a maximum of four years. The coaddition removes the possibility of probing variability on $\lesssim$1 day time scales, but pushes $\approx$1.4 magnitudes deeper than individual exposures while removing virtually all single-exposure artifacts (e.g. cosmic rays and satellites).

Approximately $\sim$30,000 of the SDSS/BOSS quasars with W1/W2 light-curves available are "IR-bright", in that they are above both the W1 and W2 single exposure thresholds and therefore detected at very high significance in the coadds. For this ensemble of objects, the typical variation in each quasar's measured (W1-W2) color is 0.06 magnitudes. This includes statistical and systematic errors which are expected to contribute variations at the few hundredths of a magnitude level. The typical measured single-band scatter is 0.07 magnitudes in each of W1 and W2.

We undertook a search for outliers relative to these trends. Specifically, we selected objects with the following characteristics:

- Monotonic variation in both W1 and W2.
- W1 versus W2 flux correlation coefficient ≥ 0.9.
- > 0.5 mag peak-to-peak variation in either W1 or W2.

This yields a sample of 248 sources. 31 of these are assumed to be blazars due to the presence of FIRST radio counterparts, and we discount them in the further analyses here. Another 22 are outside of the FIRST footprint, leaving 195 quasars in our IR-variable sample.

A link to our sample can be found here: `qso_pages_v01` and links to the catalogs are given here: `dr3_wise_lc_sample.fits.gz` and here: `dr3_wise_lc_sample.fits.gz`. The first catalog has 248 rows, which are the highly IR-variable sample of objects. The second catalog is the full 200 622 quasar sample quasars that have "good" WISE light curves available in DECaLS DR3. In each file, there are 3 extensions: the first extension are the WISE light curve summary metrics; the second extension the DECaLS DR3 data for each object, and the third extension, the SDSS data for each object. A full characterization of the typical mid-IR quasar variability will be presented separately.

Additional Multiwavelength data for J1100-0053

Checking the data archives we found there was no source within 30 arcsec in the VLA FIRST, i.e., at 21 cm radio frequencies for J11057. None of the *Hubble Space Telescope*, the *Spitzer Space Telescope* or the *Kepler* missions have observed J1100-0053. It is also not in the Hyper Suprime-Cam (HSC) Data Release 1 [5] footprint. There is the detection in ROSAT (which triggers using the 2nd all-sky survey (2RXS; Boller et al. 2016, A&A, 588, 103) as 2RXS J110058.1-005259 with 27.00 counts (count error 6.14) and a count rate = 0.06$\pm$0.01. The NASA/IPAC Extragalactic Database (NED)[2] gives J1100-0053 as $1.27 \pm 0.28 \times^{-12}$ erg/cm^2/s in the 0.1-2.4 keV range (unabsorbed flux). J1100-0053 is not in either the *Chandra* or *XMM-Newton* archives.

Further Model Details

In this section we discuss several models trying to explain the light curve and spectral behaviour of J1100-0053. Ultimately, we are forced towards a model that combines a cooling front propagating in the accretion disk along with changes in the disk opacity.

[2]https://ned.ipac.caltech.edu/

Scenario I: Obscuring Cloud model

We first explore the possibility that an obscuring cloud, or clouds, cause the observed light curve and spectral behaviour of J1100-0053. In this scenario, one would require the obscuring cloud(s) to cross the line of sight. In order to explain both the IR drop and broadline disappearance, one would also need the cloud(s) to block most of the inner disk such that the ionizing radiation could not impact on the BLR or the torus for a period of months-years. Another requirement is an explanation of why the light curves 'recover' after a period of ~ 2500 days (observed-frame); i.e., the light curves do not rapidly return to their original flux levels once the obscuring event is over.

Clouds should not typically infall; they need to lose angular momentum if they are drawn from a distribution with Keplerian orbits, and even if they do lose angular momentum, e.g., in a collision with approximately equal mass, they would likely be either destroyed or no longer coherent. Further issues arise, since the freefall timescales are,

$$t_{\rm ff} \sim 100{\rm yr}\left(\frac{\rm r}{0.4{\rm pc}}\right)^{3/2}\left(\frac{\rm M}{10^8{\rm M}_\odot}\right)^{-1} \tag{1}$$

and Kelvin-Helmholtz instabilities would destroy the clouds within the cloud-crushing time, [e.g., 7, 13, 22, 31], given by

$$t_{\rm cc} \sim 100{\rm yr}\left(\frac{\rho_{\rm cloud}/\rho_{\rm medium}}{10^6}\right)^{1/2}\left(\frac{\rm r_{cloud}}{4\times10^{10}{\rm km}}\right)\left(\frac{\rm v_{rel}}{10^4{\rm km/s}}\right)^{-1} \tag{2}$$

Thus, even if clouds did infall, they would end up fragmented, which should pollute the inner disk (see below for this discussion applied to the circumstances in Guo et al. [12]).

The dust in the cloud is then well inside the dust sublimation radius

$$R_{\rm dust} \approx 0.4{\rm pc}\left(\frac{\rm L}{10^{45}{\rm erg/s}}\right)^{1/2}\left(\frac{\rm T_{sub}}{1500{\rm K}}\right)^{2.6} \tag{3}$$

and so the dust will be destroyed in the $\sim$100 year free-fall from the dust-sublimation region. Hence, one can not absorb the UV spectrum with dust, since it will have been sublimated well before it arrives at the inner disk.

Typical extinction profiles from clouds with hydrogen column densities of $N_H \sim 10^{21} - 10^{22}{\rm cm}^{-2}$ (comparable to the range expected for NLR-BLR cloud densities) are linear in $1/\lambda$ with the 2175 Å feature, [e.g., Figure 4 of 11], and not at all like the asymptotic drop off at $1/\lambda = 3(\mu m^{-1}) = 1/300$nm in Guo et al. [12] or in our 2010 spectrum. Note that in the extinction profiles in Gordon et al. [11], there is a local maximum near $4.5 \sim 1/\lambda(\mu m^{-1})$, implying $\lambda \sim 0.2\mu$m in these cloud extinction profiles. This could correspond to broadened Lyα absorption; if this is broadened in a turbulent environment and combined with strong oxygen and carbon edges in a colder phase medium, it is possible to generate the falling off at 1/(200-300nm) in our 2010 spectrum (and Guo et al.'s spectrum). With all these considerations, we make a strong case that the behaviour observed in J1100-0053 *cannot* be extinction due to a dusty cloud.

Scenario II: Accretion Disk model

Having discounted an obscuring event as the explanation for J1100-0053, we turn to an accretion disk model.

The early 2000s spectrum is well fit with a thin, Shakura & Sunyaev [29] α-disk. The 2010 spectrum and the sharp fall-off at $\sim 200-300$nm, is not reproducible using a different temperature profile alone, even one where the entire inner disk (unphysically) vanishes. This is due to the width of the Planck function in wavelength space. For the same reasons, a gray absorber model with uniformly suppressed emission at small disk radii is also incapable of fitting our 2010 (or Guo et al.'s) spectrum. Wavelength dependent absorption, combined with a lower disk emissivity is required.

MODEL 'A': SWITCHING STATES TO AN ADAF: The broadband spectrum of NGC 1097 from Nemmen et al. [25] initially appears similar to the UV/optical 2010 spectrum of J1100-0053. In Nemmen

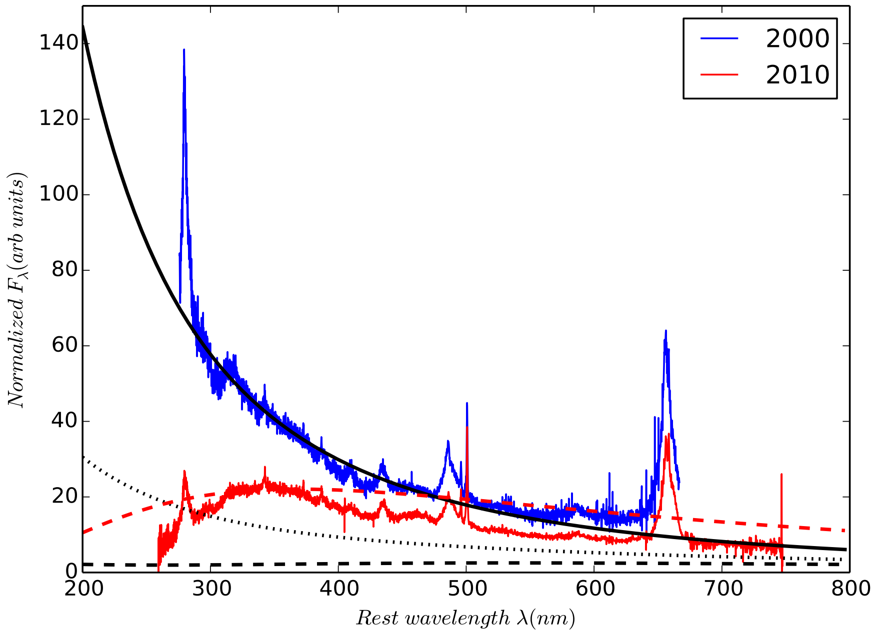

Figure 1: J1100-0053 data (blue line 2000 spectrum; red line 2010 spectrum) and 4 models. Solid black line shows non-zero torque at ISCO [following 3]; dotted and dashed black lines show temperature suppression inside $r_{\rm alt} = 225 r_{\rm g}$, such that the spectral flux is $f_{\rm dep} = 0.2$ or 0.01 (respectively) compared to a zero torque model; dashed red line shows zero flux inside $r_{\rm alt} = 80 r_{\rm g}$ and arbitrary normalization to match peak of 2010 spectrum. Note the poor fit due to the intrinsic width of the thermal peak.

et al. [25, e.g., their Figure 4], there are disk model components that look similar to the fall-off at 200nm observed in the J11057 2010 spectrum. This would involve a thin disk component extending from $\sim 450 r_g$ to the outer regions of the disk. Figure 4 in Nemmen et al. [25] shows the Multicolor Disk (MCD) blackbody-like model component from the thin disk at $r > 225 r_g$ (their long dashed line) dramatically decreasing at $\sim 10^{15}$Hz ($\sim$ 300nm). Nemmen et al. [25] model the disk region interior to this as an advection-dominated accretion flow (ADAF), at a power (in νL_ν), an order of magnitude lower than the MCD in the optical, but spanning from the X-ray to the far-IR.[3]

Can J1100-0053 switch states from a thin disk quasar to an ADAF at small radii with the thin disk surviving at large radii? Assuming the transition happens due to an instability on the thermal timescale of the disk, then at large radii the thermal timescale is

$$t_{\rm th} \sim 14 \text{ years} \left(\frac{\alpha}{0.03}\right)^{-1} \left(\frac{r}{225 r_g}\right)^{3/2} \frac{r_g}{c} \tag{4}$$

and is too long given the observations. However, if the viscosity parameter α increases to $\alpha \approx 0.3$, as suggested by King et al. [16], then the thermal timescale is $t_{\rm th} \sim 1.4$ year and the front timescale is

$$t_{\rm front} \sim 10 \text{ years} \left(\frac{h/r}{0.05}\right)^{-1} \left(\frac{\alpha}{0.3}\right)^{-1} \left(\frac{r}{225 r_g}\right)^{3/2} \frac{r_g}{c} \tag{5}$$

which is plausible, if there exists a very viscous disk and the effect propagates outwards on a timescale of ≤ 10 years from the inner disk. This would suppress the UV/X-ray emission from the RIAF (down by a few orders of magnitude from the intensity expected from a thin disk intensity) and explain the broadline behaviour. ADAF spectra are flat in νL_ν Abramowicz & Fragile [1], Abramowicz et al. [2], Narayan

[3] A change to a radiatively inefficient accretion flow (RIAF) is also possible in this model.

et al. [24], and convective ADAFs rise towards X-ray energies. ADAFs exist at lower luminosity, where $\varepsilon \sim 0.005$ for $L = \varepsilon \dot{M} c^2$, lower than the fiducial $\varepsilon \sim 0.1$ for a classic thin disk luminosity.

However, suppressing the flux from the inner disk radii ($\lesssim 225 r_g$) in the low temperature thin disk model [3, 4, 9, 10, 23], by a factor of 20 would still not describe the 2010 spectrum. To restore the thin disk spectrum by 2016, the disk change has to propagate back inwards, most of the way to the ISCO and therefore $t_{\rm front}$ needs to be shorter. This requires h/r to be larger in Equation above, by a factor of ~ 2.

It is unclear what physical processes would trigger the change of state to an ADAF and then cool back down to a thin disk. However, more of an issue is that supressing the MCD temperature profile inside a radius of $r_{alt} = 225 r_g$ leads to a collapse in the total flux compared to unperturbed disk. We show some example cases in 1. Clearly, these scenarios are difficult to reconcile with our data.

MODEL 'B': PROPAGATING OF A COOLING FRONT: An alternative model connected to the accretion disk is that a *cooling* front propagates through the thin disk. In order to reproduce the steep fall at $\lambda \leq 200$nm in the 2010 spectrum, a cool phase leads to absorption at short wavelengths.

Initially a modestly fat disk ($h/r \sim 0.2$) with a modest α, cools from the ISCO and propagates outward in a cooling front, collapsing the disk. As the hot disk ($\sim 10^{5-6}$K) cools, it fragments into cooler clumps around $\sim 10^4$K [see e.g., 19]. The main coolants are resonance lines in carbon and oxygen [see e.g., Fig. 18 in 34] The ionization energies for carbon and carbon are 11.26 and 13.61 eV, respectively, i.e., $\sim$ 100nm, and hence at wavelengths $<$ 100nm the disk opacity will increase dramatically in an edge. However, the gas in the disk is both pressure, turbulent and Doppler broadened, so these ionization edges will manifest around 100nm with decreasing opacity to shorter wavelengths as

$$\kappa \propto \rho T^{-1/2} \nu^{-3} \tag{6}$$

for Kramers' opacities. This implies $\kappa \propto \lambda^3$ at increasing wavelengths up to the ionization edge around 100nm. These features will be blurred (by the broadening) and the ionization edges due to the C and O resonance lines in the cool phase of this disk will be span $50 - 200$nm, depressing the flux at these energies.

The 2010 spectrum in this model comes from a cooler disk plus the increased opacity at short wavelengths in the cooler phase. Heating occurs from the outside in, explaining the 2016 spectrum and asymmetric recovery in photometry. Since the optical continuum has been rising again since mid-2016, this leads to a prediction of a rise in hydrogen emission line flux in the next few months (2018). The infrared flux returns in 2021.

Comparison with SDSS J2317+0005 from Guo et al. 2016

Figure 1 of Guo et al. (2016) shows a UV collapse in the quasar SDSS J231742.60+000535.1 (hereafter J2317+0005, with redshift $z = 0.32$), similar to that of J1100-0053. In Figure 2 we show the five SDSS/BOSS spectra from J1100-0053 and J2317+0005 (top panel), and their ratios (bottom panel). The collapse in J2317+0005 happens in 23 days [Figure 2 of 12]; this object was observed by SDSS on MJD 52177 (normal) and then on MJD 52200. In the second epoch spectrum, there is a drop of 1.2 mag in the u-band and 0.5mag in g-band. The r, i, z-bands are all consistent with the earlier observation. J2317+0005 is observed with SDSS $\sim$a year later and (u, g, r, i, z) are all consistent with the earlier MJD 52177 spectrum. XMM-Newton spectra straddle this time period, from 2001 June 03 to 2001 November 28. Both X-ray spectra are consistent with no neutral absorption in the rest-frame. This implies the sightline is clear on both of those dates. Guo et al. [12] also find that the IR does not significantly change and that the broad lines are consistent with being constant over time.

Guo et al. [12] discuss two scenarios to explain this behaviour: *(i)* an inner accretion disk change and *(ii)* an eclipse by an optically thick cloud. Guo et al. [12] note that in principle both models could explain the observation. In the inner accretion disk scenario, turning off the disk at $r < 60 r_{\rm g}$ would explain the J2317+0005 spectra, though the detailed MCD fit is far from ideal, in much the same manner as for J11057. However, Guo et al. [12] find this explanation unconvincing since "quasars are not observed to flicker like this typically". The second scenario is favoured based on the initial optical spectrum (23 days before the u-band dip) and the 2001 November X-ray spectrum (45 days after the u-band dip). For the

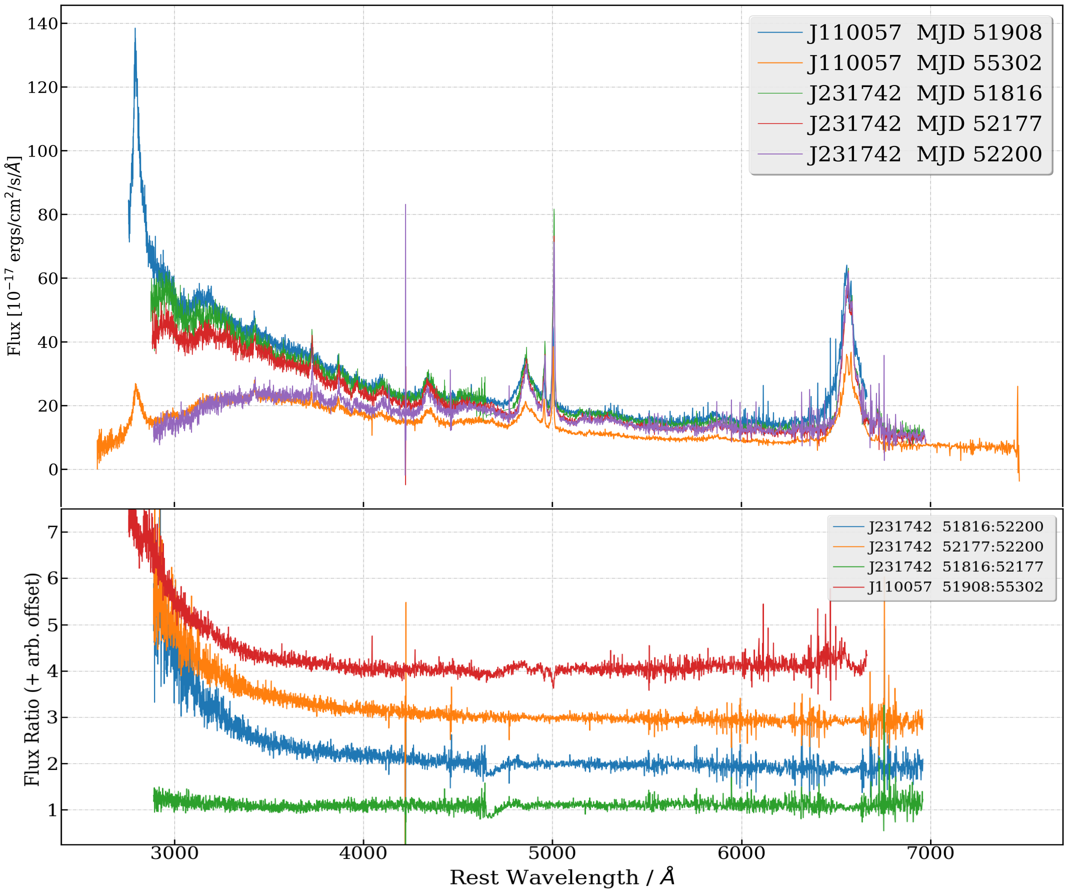

Figure 2: *Top::* The five SDSS/BOSS spectra of J2317+0005 and J1100-0053. The striking similarity between the two spectra downturned in the blue can be seen. *Bottom::* The ratio of the different epoch spectra.

reasons given above for J1100-0053, and in particular with our infrared light curve data, we suggest ≈45 days is too short for an obscuration event, and hence suggest that the same initial cause (model B above: a cooling front propagating from the inner accretion disk) explains *both* the Guo et al. [12] spectrum and our 2010 spectrum. In the case of the Guo et al. [12] source, the fact that the IR and broad lines are unchanged implies that the temporary disk dimming is very short-lived. Therefore, in the case of Guo et al. [12], the restoring heating front must propagate outwards from the inner disk. This is unlike J1100-0053 (model B above), where the restoring heating front must propagate inwards from the outer disk in order to explain the restoration of g-band before u-band and the long-term supression of broad lines and IR.

Acknowledgements

NPR acknowledges support from the STFC and the Ernest Ruther- ford Fellowship scheme. KESF & BM are supported by NSF PAARE AST-1153335. KESF & BM thank CalTech/JPL for support during sabbatical. MF acknowledges support from NSF grants AST-1518308, AST-1749235, AST-1413600 and NASA grant 16-ADAP16-0232.

Funding for SDSS-III has been provided by the Alfred P. Sloan Foundation, the Participating Institutions, the National Science Foundation, and the U.S. Department of Energy Office of Science. The SDSS-III web site is http://www.sdss3.org/.

SDSS-III is managed by the Astrophysical Research Consortium for the Participating Institutions of the SDSS-III Collaboration including the University of Arizona, the Brazilian Participation Group, Brookhaven National Laboratory, Carnegie Mellon University, University of Florida, the French Participation Group, the German Participation Group, Harvard University, the Instituto de Astrofisica de Canarias, the Michigan State/Notre Dame/JINA Participation Group, Johns Hopkins University, Lawrence Berkeley National Laboratory, Max Planck Institute for Astrophysics, Max Planck Institute for Extraterrestrial Physics, New Mexico State University, New York University, Ohio State University, Pennsylvania State University, University of Portsmouth, Princeton University, the Spanish Participation Group, University of Tokyo, University of Utah, Vanderbilt University, University of Virginia, University of Washington, and Yale University.

This publication makes use of data products from the Wide-field Infrared Survey Explorer, which is a joint project of the University of California, Los Angeles, and the Jet Propulsion Laboratory/California Institute of Technology, and NEOWISE, which is a project of the Jet Propulsion Laboratory/California Institute of Technology. WISE and NEOWISE are funded by the National Aeronautics and Space Administration.

This research has made use of the NASA/IPAC Extragalactic Database (NED) which is operated by the Jet Propulsion Laboratory, California Institute of Technology, under contract with the National Aeronautics and Space Administration.

References

[1] Abramowicz M. A., Fragile P. C., 2013, Living Reviews in Relativity, 16, 1

[2] Abramowicz M. A., Igumenshchev I. V., Quataert E., Narayan R., 2002, ApJ, 565, 1101

[3] Afshordi N., Paczyński B., 2003, ApJ, 592, 354

[4] Agol E., Krolik J. H., 2000, ApJ, 528, 161

[5] Aihara H., et al., 2017, ArXiv e-prints

[6] Appenzeller I., et al., 1998, ApJS, 117, 319

[7] Bae H.-J., Woo J.-H., 2016, ApJ, 828, 97

[8] Dawson K., et al., 2013, AJ, 145, 10

[9] Ford K. E. S., et al., 2018, in prep.

[10] Gammie C. F., 1999, ApJ Lett., 522, L57

[11] Gordon K. D., Clayton G. C., Misselt K. A., Landolt A. U., Wolff M. J., 2003, ApJ, 594, 279

[12] Guo H., et al., 2016, ApJ, 826, 186

[13] Hopkins P. F., 2013, MNRAS, 428, 2840

[14] Kepler S. O., et al., 2015, MNRAS, 446, 4078

[15] Kepler S. O., et al., 2016, MNRAS, 455, 3413

[16] King A. R., Pringle J. E., Livio M., 2007, MNRAS, 376, 1740

[17] Lang D., 2014, AJ, 147, 108

[18] Margala D., Kirkby D., Dawson K., Bailey S., Blanton M., Schneider D. P., 2016, ApJ, 831, 157

[19] McCourt M., Oh S. P., O'Leary R. M., Madigan A.-M., 2016, ArXiv e-prints

[20] Meisner A. M., Bromley B. C., Nugent P. E., Schlegel D. J., Kenyon S. J., Schlafly E. F., Dawson K. S., 2017, AJ, 153, 65

[21] Meisner A. M., Lang D., Schlegel D. J., 2017, AJ, 154, 161

[22] Nagakura H., Yamada S., 2008, ApJ, 689, 391

[23] Narayan R., Kato S., Honma F., 1997, ApJ, 476, 49

[24] Narayan R., Mahadevan R., Quataert E., 1998, in Abramowicz M. A., Björnsson G., Pringle J. E., eds, Theory of Black Hole Accretion Disks Advection-dominated accretion around black holes. pp 148–182

[25] Nemmen R. S., Storchi-Bergmann T., Yuan F., Eracleous M., Terashima Y., Wilson A. S., 2006, ApJ, 643, 652

[26] Richards G. T., et al., 2002, AJ, 123, 2945

[27] Ross N. P., et al., 2012, ApJS, 199, 3

[28] Schneider D. P., et al., 2002, AJ, 123, 567

[29] Shakura N. I., Sunyaev R. A., 1973, Astron. & Astrophys., 24, 337

[30] Shen Y., et al., 2011, ApJS, 194, 45

[31] Shiokawa H., Krolik J. H., Cheng R. M., Piran T., Noble S. C., 2015, ApJ, 804, 85

[32] Stoughton C., et al., 2002a, AJ, 123, 485

[33] Stoughton C., et al., 2002b, AJ, 123, 485

[34] Sutherland R. S., Dopita M. A., 1993, ApJS, 88, 253

[35] Voges W., et al., 1999, Astron. & Astrophys., 349, 389